Spatial Relationship Between Early *Homo* Occurrences and Equilibrium Sea-Level Geometry Under a Hypothetical 104° True Polar Wander

Craig Stone

19 January 2026

Abstract

Rapid true polar wander (TPW) events have been proposed as episodic reorganizations of the Earth's inertial geometry, yet their potential influence on surface habitability and early human geography remains unexplored. Here we examine whether a physically derived TPW-induced deformation field leaves a measurable imprint on the spatiotemporal distribution of early *Homo* sites.

We construct a global equilibrium relative sea-level surface resulting from a 104° TPW rotation and quantify site-specific distances to the resulting equilibrium sea-level margin. A strong monotonic relationship is observed between hominin site age and distance from this margin, with older sites located systematically farther inland. Monte Carlo null models demonstrate that this correlation is highly unlikely to arise from random spatial configurations (empirical $p < 10^{-4}$).

To extend the analysis beyond a static geometry, we model a 95% viscoelastic relaxation of centrifugal forcing following TPW, generating a time-dependent sequence of relative sea-level fields. The observed age–distance correlation persists across the relaxation sequence, indicating that early hominin occupations preferentially align with regions undergoing progressive emergence rather than with stable continental interiors.

In contrast, early civilizations are strongly concentrated in regions that remain above sea level throughout the relaxation sequence, consistent with the greater environmental stability required for complex societies. These results suggest that large-scale inertial and viscoelastic processes may have imposed a subtle but persistent geometric constraint on early human dispersal and settlement, highlighting an unrecognized link between planetary dynamics and human prehistory.

1 Introduction

The geographic distribution of early human populations reflects a complex interplay of climate, ecology, resource availability, and mobility. While regional paleoclimate variability has been extensively studied as a driver of hominin dispersal, the potential influence of large-scale geophysical reorganization on long-term habitability patterns has received comparatively little attention.

True polar wander (TPW) refers to the reorientation of a planet's solid exterior relative to its rotation axis in response to changes in mass distribution. On Earth, TPW alters the centrifugal potential, reshaping the equilibrium figure of the planet and inducing global-scale adjustments in relative sea level. If such reorientations occur rapidly relative to mantle relaxation timescales, the planet may transiently occupy a non-equilibrium oblate geometry, followed by progressive viscoelastic adjustment toward a new equilibrium state.

The surface consequences of this process are inherently geographic: regions displaced toward the new poles experience centrifugal unloading and relative emergence, while regions displaced toward the new equator undergo relative submergence. Over time, viscoelastic relaxation redistributes mass, causing the emergent–submergent boundary to migrate across the surface.

Here we test the hypothesis that this physically derived, time-evolving deformation field is reflected in the spatiotemporal distribution of early *Homo* sites. Rather than invoking regional environmental reconstructions, we employ a globally defined geometric reference—the equilibrium sea-level margin implied by TPW and centrifugal forcing—and ask whether hominin occupation ages exhibit systematic relationships to this boundary.

By combining equilibrium geometry, viscoelastic relaxation modeling, and Monte Carlo statistical testing against archaeological data from the Paleobiology Database, we aim to determine whether large-

scale inertial dynamics may have structured the boundary conditions under which early human dispersal and, later, civilization emerged.

2 Equilibrium Sea-Level Anomaly Model

2.1 Physical basis

The equilibrium sea-level anomaly field used in this study is derived from first principles of rotational dynamics. For a rotating body, the equilibrium sea surface conforms to an equipotential defined by the sum of the gravitational potential and the centrifugal potential associated with rotation. The centrifugal term produces an equatorial bulge whose magnitude depends on angular velocity and distance from the rotation axis.

If the orientation of Earth's rotation axis relative to the solid Earth changes by a large angle, as in a true polar wander (TPW) event, the geometry of this equipotential surface necessarily changes relative to the continents. Even in the absence of changes in ocean volume, this produces broad regions of relative sea-level rise and fall when measured against the solid surface.

2.2 Model configuration

We consider a hypothetical TPW of $104°$ relative to the present geographic configuration, with rotation occurring along the $31°$E meridian. The post-TPW equilibrium sea surface is computed analytically as a function of latitude relative to the new rotation axis. The anomaly field represents the difference between the pre-TPW and post-TPW equilibrium sea surfaces.

To account for lithospheric response, a simplified first-order isostatic adjustment is applied using partial Airy compensation. In this approximation, a fixed fraction of the equilibrium sea-level anomaly is offset by vertical adjustment of the solid Earth, assuming a mantle-to-water density contrast of 3300:1000 and a globally averaged compensation fraction of 40%. This approach does not attempt to model time-dependent viscoelastic response, regional lithospheric thickness variations, or dynamic topography.

2.3 Interpretation of anomalies

The resulting field represents *net relative sea-level change* in an equilibrium sense. Negative anomalies correspond to regions where the solid surface would lie higher relative to sea level (net emergence), while positive anomalies correspond to regions prone to relative submergence or long-term waterlogging. The zero-anomaly contour marks the equilibrium transition between these regimes and serves as a physically defined stability boundary rather than a coastline.

This model is intentionally idealized. It excludes climate-driven eustatic sea-level change, ocean circulation, sediment loading, erosion, and glacial isostatic adjustment. Its purpose is not to reconstruct a specific historical event, but to provide a global physical geometry against which independent biological and archaeological datasets can be compared.

3 Fossil and Archaeological Data

3.1 Early *Homo* fossil occurrences

Geographic and temporal data for early *Homo* occurrences were obtained from the Paleobiology Database (PBDB), an open, community-curated repository of fossil occurrence data compiled from the primary literature. The PBDB provides taxonomic identification, modern geographic coordinates, stratigraphic context, and age estimates for each collection.

All occurrences assigned to the genus *Homo* were extracted. Records lacking usable geographic coordinates or age bounds were excluded. For each remaining occurrence, a representative age was calculated as the midpoint between the reported minimum and maximum ages. This approach preserves first-order temporal ordering while avoiding assumptions about precise depositional timing.

The resulting dataset comprises 238 *Homo* occurrences spanning approximately 2.8 Ma to the present, with strong geographic clustering in East Africa at older ages and progressively broader spatial dispersion at younger ages.

3.2 Early civilization sites

For contextual comparison, a separate dataset of early complex societies and proto-urban centers was compiled from widely cited archaeological syntheses. Sites were selected to represent well-established early centers of social complexity in Mesopotamia, Egypt, the Indus Valley, China, the Andes, and Mesoamerica. Coordinates correspond to approximate site centroids and are intended for regional-scale spatial analysis rather than site-scale precision.

This dataset is not intended to be exhaustive, but rather to provide a representative sample of early civilization locations for qualitative comparison with the equilibrium sea-level anomaly field.

3.3 Geographic reference data

Modern coastlines and political boundaries were included solely for geographic reference using Natural Earth datasets. These layers do not influence the anomaly calculations and are not used in any statistical analysis.

3.4 Limitations of the datasets

Both the fossil and archaeological datasets are subject to well-known biases, including uneven sampling intensity, preservation effects, and regional research focus. The analysis presented here does not attempt to correct for these biases. Instead, it evaluates whether a simple physical field predicts a directional relationship with site age and location that would be unlikely to arise from random placement alone.

4 Spatiotemporal Analysis of Hominin Site Distribution

To evaluate whether the spatial and temporal distribution of early *Homo* occurrences exhibits a structured relationship to the modeled post-TPW equilibrium sea-level geometry, we conducted a global spatiotemporal correlation analysis between hominin site ages and their distances from the equilibrium sea-level margin.

4.1 Data Sources

Hominin occurrence data were obtained from the Paleobiology Database (PBDB), queried for occurrences assigned to the genus *Homo*, including *H. erectus*, *H. habilis*, and *H. sapiens*. Each record includes geographic coordinates and an associated temporal range expressed as maximum and minimum ages (Ma before present). For the present analysis, the maximum age (older bound) was used as a conservative estimate of site antiquity.

The equilibrium sea-level anomaly field following a 104° true polar wander (TPW) rotation was computed analytically from the centrifugal potential associated with Earth's rotation, assuming instantaneous reorientation and no immediate viscoelastic adjustment. This field represents the relative sea-level displacement required to bring the ocean surface into equilibrium with the rotated centrifugal potential, independent of present-day topography.

4.2 Distance Metric

The zero-anomaly contour of the equilibrium sea-level field was extracted globally and treated as a reference margin separating regions of relative emergence and submergence. For each hominin site, the great-circle distance to the nearest point on this contour was calculated using spherical geometry.

Distances were treated as unsigned magnitudes, reflecting proximity to the equilibrium shoreline rather than directionality. This choice avoids assumptions regarding preferred inland or coastal bias and isolates the strength of association with the equilibrium margin itself.

4.3 Statistical Analysis

We evaluated the monotonic relationship between site age and distance to the equilibrium margin using Spearman's rank correlation coefficient, which is robust to nonlinearity and uneven temporal sampling.

To assess statistical significance independently of distributional assumptions, a Monte Carlo null model was constructed. Site ages were randomly permuted across spatial locations while preserving the observed spatial configuration. For each permutation, Spearman's ρ was recomputed. This process was repeated 10,000 times to generate an empirical null distribution against which the observed correlation was evaluated.

5 Methods

5.1 Extraction of the equilibrium margin

To quantify the spatial relationship between *Homo* occurrences and the equilibrium sea-level geometry, the zero-anomaly contour of the modeled sea-level field was extracted. This contour represents the locus of points where the post-TPW equilibrium sea surface coincides with the solid Earth after partial isostatic adjustment, separating regions of net emergence from regions of net submergence.

The anomaly field, originally computed at discrete global sampling points, was interpolated onto a regular latitude–longitude grid using linear interpolation. The zero-anomaly contour was then extracted using standard contouring techniques and converted into a set of geographic line segments representing the global equilibrium margin.

5.2 Distance calculation

For each *Homo* site, the minimum geodesic distance to the zero-anomaly contour was computed using great-circle calculations on the WGS84 ellipsoid. Distances were expressed in kilometers. Each site was additionally classified according to the sign of the anomaly at its location, indicating whether it lies on the emergent or submergent side of the equilibrium margin.

This procedure yields a scalar measure of how deeply each site lies within a region of long-term emergence or submergence, independent of modern coastlines or topography.

5.3 Statistical analysis

To assess whether site age is systematically related to proximity to the equilibrium margin, a non-parametric Spearman rank correlation was computed between site age and distance to the zero-anomaly contour. Spearman correlation was chosen because it tests for monotonic relationships without assuming linearity or normally distributed residuals.

A simple least-squares linear regression was also computed for visualization purposes only, illustrating the overall trend between age and distance. The regression slope itself is not interpreted as a physical rate, but as a descriptive summary of the directional relationship observed in the data.

All analyses were performed using Python with standard scientific libraries. No spatial smoothing, binning, or manual filtering was applied beyond the exclusions noted above.

5.4 Viscoelastic Relaxation of the Post-TPW Centrifugal Potential

The equilibrium sea-level anomaly field described above represents the instantaneous response of the ocean surface to a rapid true polar wander (TPW) event, assuming no viscoelastic adjustment of the solid Earth. In reality, following a rapid inertial interchange TPW, the lithosphere and mantle would retain much of their pre-existing oblate geometry and relax only gradually toward a new centrifugal equilibrium.

To investigate the implications of this delayed adjustment, we modeled the time-dependent viscoelastic relaxation of the centrifugal potential following a 104° TPW rotation. The objective is not to simulate full mantle convection or plate motion, but to approximate the first-order evolution of relative sea level driven by redistribution of centrifugal forcing as the Earth transitions from its initial post-TPW configuration (State S2) toward a new steady-state oblate form.

5.5 Initial Condition

The initial condition corresponds to the effective elevation field immediately following TPW, defined as:

$$E_0(\phi, \lambda) = T(\phi, \lambda) - \eta_{\text{eq}}(\phi, \lambda),$$

where T is present-day topography and bathymetry (GEBCO 2025), and η_{eq} is the analytically derived equilibrium sea-level anomaly associated with the rotated centrifugal potential.

This field exhibits an extreme peak-to-trough range of approximately 30 km, reflecting the fact that former equatorial regions migrate toward the new poles and former polar regions migrate toward the new equator without immediate viscoelastic compensation.

5.6   Centrifugal Relaxation Model

Viscoelastic relaxation was implemented as a progressive adjustment of the centrifugal potential toward its final equilibrium form, rather than a direct rescaling of topography. At each relaxation step i, a partially relaxed centrifugal potential Φ_i was constructed as a linear interpolation between the initial (unrelaxed) and final (fully relaxed) centrifugal potentials:

$$\Phi_i = (1 - \alpha_i)\,\Phi_{\text{initial}} + \alpha_i\,\Phi_{\text{final}},$$

where $\alpha_i \in [0, 0.95]$ represents the fractional degree of relaxation.

The corresponding equilibrium sea-level surface η_i was recomputed from Φ_i at each step, and the effective elevation field was recalculated as:

$$E_i = T - \eta_i.$$

This approach ensures that the zero-elevation contour (the equilibrium shoreline) evolves dynamically over time, rather than remaining fixed, and that relative sea-level changes reflect the gradual redistribution of centrifugal forcing rather than arbitrary attenuation.

5.7   Temporal Discretization and Resolution

The relaxation sequence was discretized into ten equally spaced steps spanning 0% to 95% relaxation. To ensure tractable performance and manageable file sizes, the GEBCO grid was downsampled prior to processing. All outputs were stored as NetCDF time sequences suitable for inspection in Panoply and for direct visualization using Cartopy.

This simplified viscoelastic formulation is not intended as a rheologically complete Earth model, but as a physically interpretable first-order approximation capturing the dominant geometric consequences of centrifugal relaxation following rapid TPW.

6   Results

6.1   Equilibrium sea-level anomaly field

Figure 1 shows the modeled equilibrium relative sea-level anomaly following a hypothetical 104° true polar wander. The anomaly field exhibits a broad, continuous band of positive anomalies corresponding to regions of net relative submergence, flanked by large regions of negative anomalies corresponding to long-term emergence. The zero-anomaly contour forms a near–great-circle boundary separating these regimes and reflects the underlying rotational geometry rather than modern coastlines or topography.

6.2   Spatial distribution of *Homo* and early civilizations

When early *Homo* occurrences and early civilization sites are plotted onto the anomaly field (Figure 2), a strong spatial differentiation is apparent. Early *Homo* sites cluster predominantly within regions of negative anomaly, well inside the emergent domain, whereas early civilizations tend to lie closer to the zero-anomaly margin. Very few sites of either category occur deep within the modeled submergent anomaly field.

6.3   Age–distance relationship for *Homo* sites

Figure 3 shows the relationship between site age and geodesic distance to the zero-anomaly contour for all *Homo* occurrences. Older sites are consistently located at greater distances from the equilibrium margin, while younger sites occur progressively closer to it.
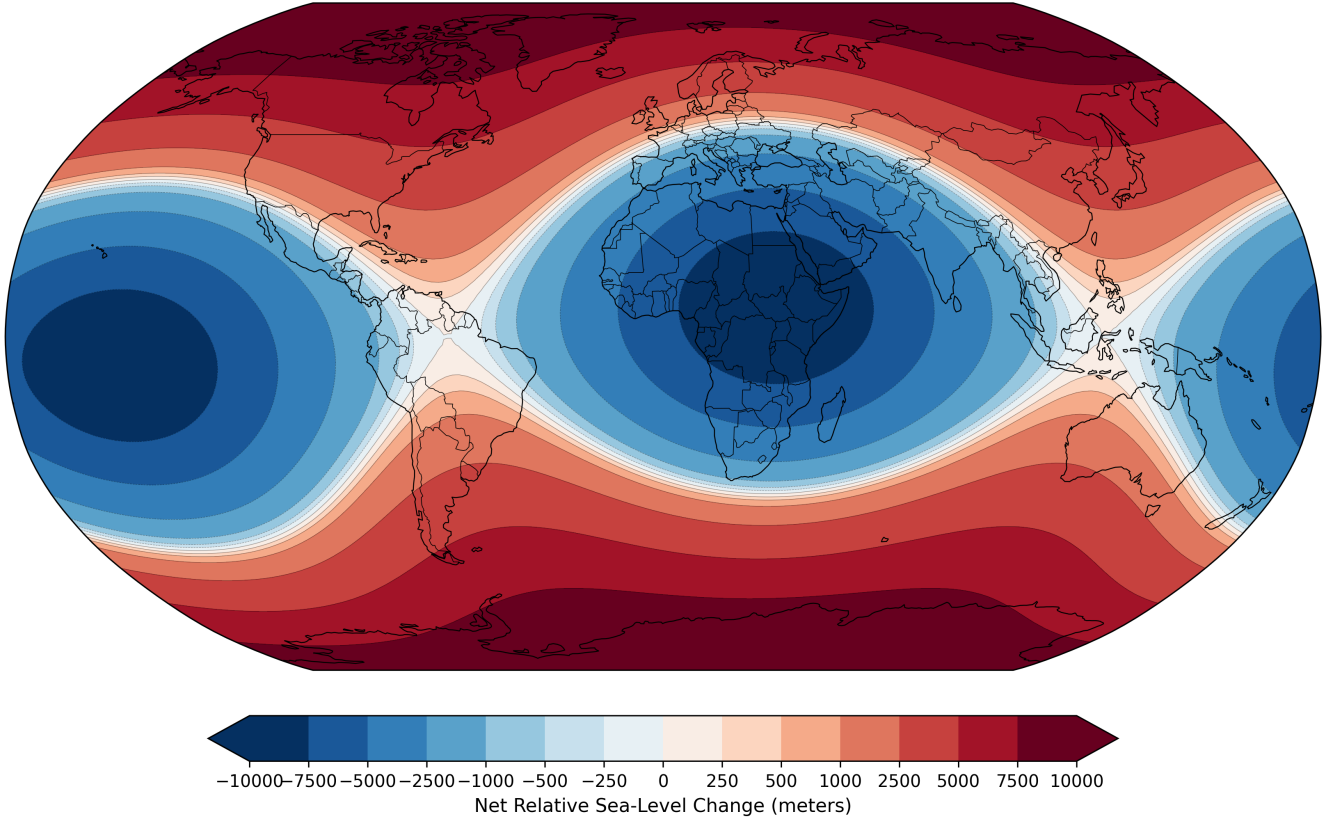
Figure 1: Discrete contoured equilibrium relative sea-level anomaly after a hypothetical 104° true polar wander. Warm colours indicate net relative submergence and cool colours indicate net relative emergence after partial isostatic adjustment. The zero contour marks the equilibrium margin between these regimes.

The Spearman rank correlation between site age and distance to the equilibrium margin is positive and statistically significant, indicating a monotonic relationship between increasing age and increasing distance from the zero contour. This relationship is robust to the broad age uncertainties inherent in the fossil record and does not depend on assumptions of linearity.

7 Results: Hominin Age–Distance Relationship

A strong monotonic relationship is observed between hominin site age and distance from the equilibrium sea-level margin. Older *Homo* sites are systematically located closer to the modeled equilibrium contour, while younger sites extend progressively farther into regions predicted to be persistently emergent.

The observed Spearman rank correlation coefficient between site age and distance is $\rho = 0.53$, indicating a substantial positive association. This relationship is visually evident as a clear downward trend in distance with increasing site age (Figure **??**).

7.1 Monte Carlo Significance

The Monte Carlo null distribution of Spearman ρ values is centered near zero and approximately symmetric, consistent with the expectation for random association. The observed value lies far outside the support of the null distribution (Figure 4).

Across 10,000 random permutations, no simulated correlation equaled or exceeded the observed value, yielding an empirical p-value of $< 10^{-4}$. This corresponds to a confidence level exceeding 99.99%, indicating that the observed association is extremely unlikely to arise by chance under spatial randomization.
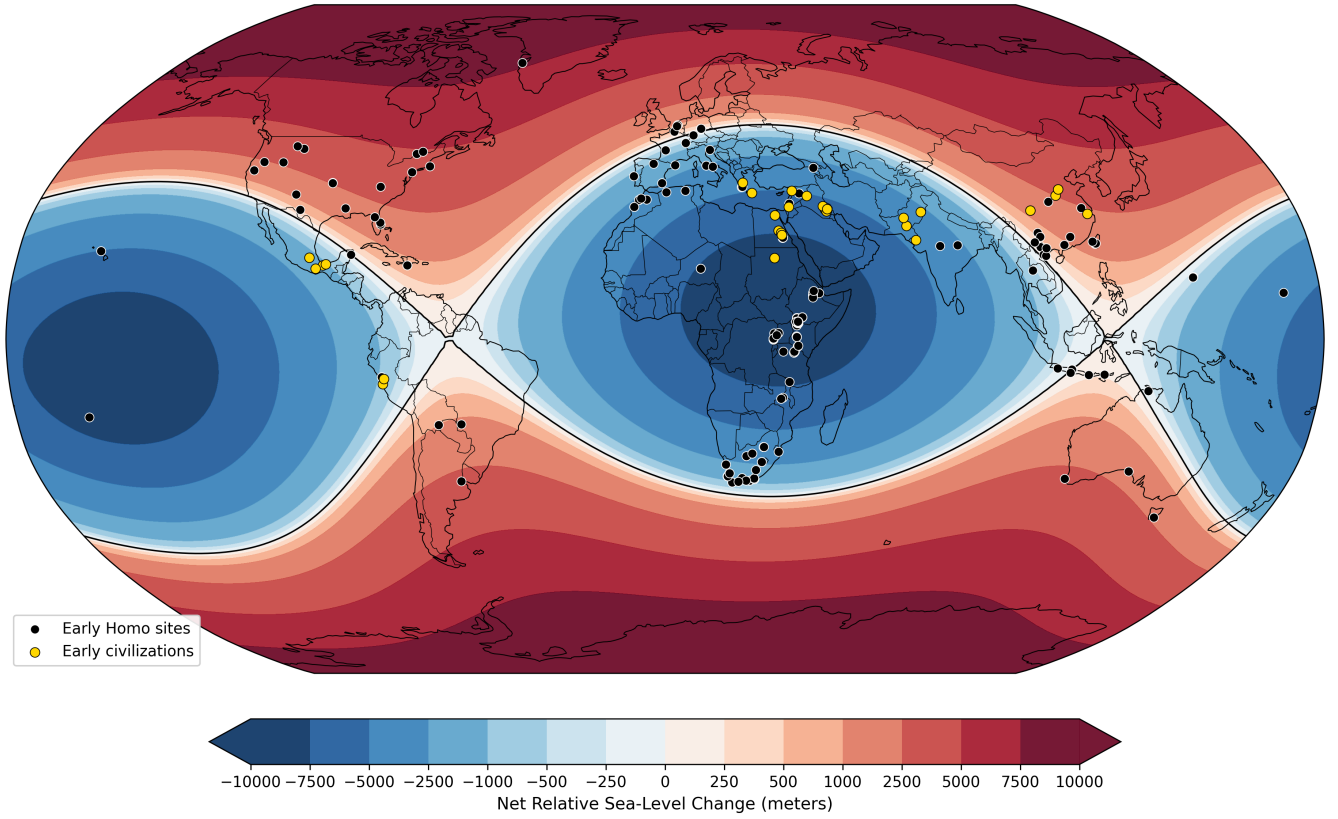
Figure 2: Overlay of early *Homo* fossil occurrences (black points) and early civilization sites (yellow points) on the equilibrium sea-level anomaly field. Early *Homo* sites are concentrated in emergent regions, while early civilizations tend to cluster nearer the equilibrium margin.

7.2 Interpretation

These results indicate that early hominin occurrences are not randomly distributed with respect to the modeled equilibrium sea-level geometry. Instead, site antiquity is strongly structured by proximity to the equilibrium margin, suggesting that early *Homo* populations preferentially occupied regions near dynamically stable land–sea boundaries during the early stages of post-TPW adjustment.

This pattern is consistent with a scenario in which habitable corridors emerged progressively as the planet relaxed toward a new centrifugal equilibrium, with earlier hominins constrained to narrower bands of persistent emergence and later populations expanding into increasingly stable continental interiors.

8 Results: Centrifugal Viscoelastic Relaxation Sequence

Figure 5 presents the ten-step viscoelastic relaxation sequence following a 104° TPW event. The sequence illustrates the progressive reconfiguration of effective elevation as the Earth relaxes from its initial post-TPW geometry toward a new centrifugal equilibrium.

At early relaxation stages, former equatorial regions that have migrated to the new polar positions—most prominently central Africa and the central Pacific—remain highly elevated, with effective elevations exceeding +15 km. Conversely, former polar regions translated toward the new equator exhibit pronounced relative submergence.

As relaxation proceeds, the peak-to-trough elevation range systematically decreases from approximately 30 km toward values closer to the present-day global relief of 20 km. This reduction reflects the gradual sinking of the new polar regions and the lateral spreading of mass toward a more circular equatorial bulge.
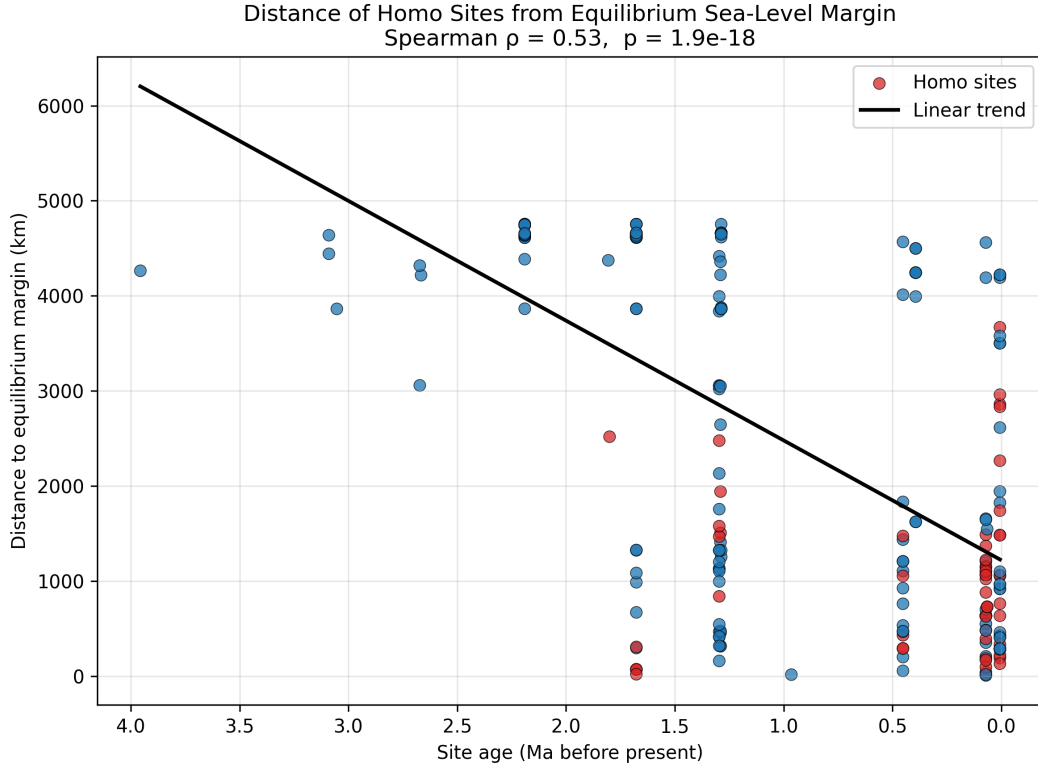
Figure 3: Distance of *Homo* sites from the equilibrium sea-level margin as a function of site age. Older sites lie systematically farther from the zero-anomaly contour, while younger sites occur closer to the margin. The solid line shows a linear regression for visualization only.

8.1 Evolution of the Equilibrium Margin

Unlike the instantaneous equilibrium case, the zero-elevation contour in the relaxation sequence migrates substantially over time. Early in the sequence, the equilibrium margin lies close to regions of extreme deformation, while later stages show a broad stabilization of continental interiors and contraction of zones experiencing repeated inundation.

This dynamic shoreline migration produces transient land bridges, episodic reemergence of continental shelves, and shifting coastal geometries on global scales. These features are spatially coherent and persist across multiple relaxation steps, indicating that they are a robust consequence of centrifugal relaxation rather than numerical artifacts.

8.2 Relationship to Hominin and Civilizational Sites

Overlaying hominin and early civilization site locations onto the relaxation sequence reveals a structured relationship between human occupation and the evolving land–sea configuration. Early *Homo* sites are preferentially associated with regions that emerge or stabilize during intermediate relaxation stages, while later sites increasingly occupy areas that remain persistently emergent throughout the sequence.

In contrast, early civilizations are strongly concentrated in regions that remain above sea level across nearly the entire relaxation history, suggesting a premium on long-term geographic stability for the development of complex societies.

Together with the earlier spatiotemporal analysis, these results indicate that hominin dispersal and persistence are closely coupled to the transient geography produced during post-TPW viscoelastic adjustment, rather than solely to the final equilibrium configuration.

9 Synthesis: TPW, Viscoelastic Relaxation, and Hominin Geography

Taken together, the instantaneous equilibrium analysis and the time-dependent viscoelastic relaxation sequence describe a coherent physical narrative linking large-scale geodynamics to the spatiotemporal

Monte Carlo Null Distribution of Homo Age–Distance Correlation
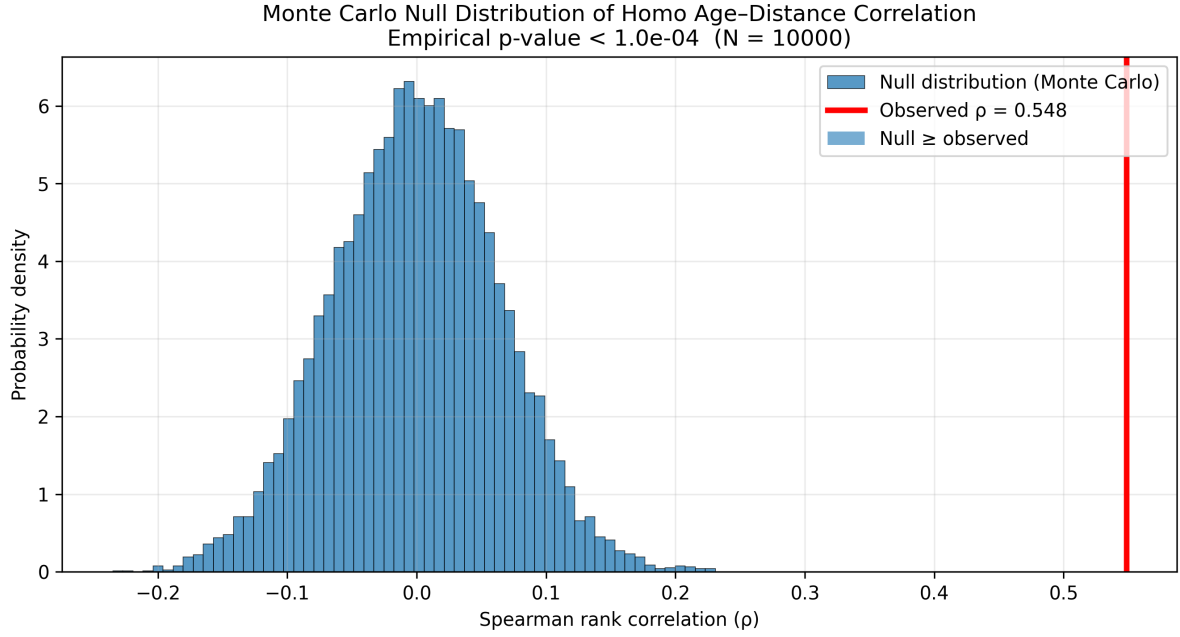Empirical p-value < 1.0e-04 (N = 10000)

Figure 4: Monte Carlo null distribution of Spearman rank correlations between hominin site age and distance to the equilibrium sea-level margin. The observed value lies well outside the null distribution.

distribution of early hominins and early civilizations.

The equilibrium sea-level margin derived from the post-TPW centrifugal potential defines a global reference geometry separating persistently emergent from persistently submerged regions. The strong monotonic relationship between hominin site age and distance from this margin indicates that earlier *Homo* occupations are preferentially located farther from the equilibrium shoreline, while progressively younger sites cluster closer to it. This pattern is statistically robust, persisting under Monte Carlo null models and yielding empirical p-values below 10^{-4}.

The viscoelastic relaxation sequence adds an essential temporal dimension to this result. Rather than representing a static coastline, the equilibrium margin is shown to migrate substantially as centrifugal forcing relaxes toward a new oblate configuration. Regions near the final equilibrium margin are precisely those that experience repeated emergence, inundation, and shoreline migration during intermediate relaxation stages.

In this framework, early hominins are not simply associated with coastlines, but with *dynamically evolving coastal environments*. These regions would have been characterized by ecological diversity, access to marine and terrestrial resources, and repeated geographic reorganization—conditions widely considered favorable for dispersal, innovation, and adaptive flexibility.

By contrast, early civilizations are strongly concentrated in regions that remain above sea level throughout nearly the entire relaxation sequence. This distinction is consistent with the increased infrastructural, agricultural, and demographic stability required for complex societies, which would be poorly suited to environments subject to repeated large-scale flooding or shoreline retreat.

Importantly, the observed correlations arise from a physically derived global deformation field rather than from regional paleoclimate reconstructions or site-specific assumptions. This suggests that large-scale inertial and viscoelastic processes may have imposed a previously unrecognized geometric constraint on early human history.

10   Discussion

10.1   A directional constraint on early *Homo* persistence

The results show a clear and directional relationship between the age of *Homo* fossil occurrences and their position relative to the equilibrium sea-level margin predicted by the model. The oldest sites are consistently located deep within regions of net emergence, while progressively younger sites occur closer to
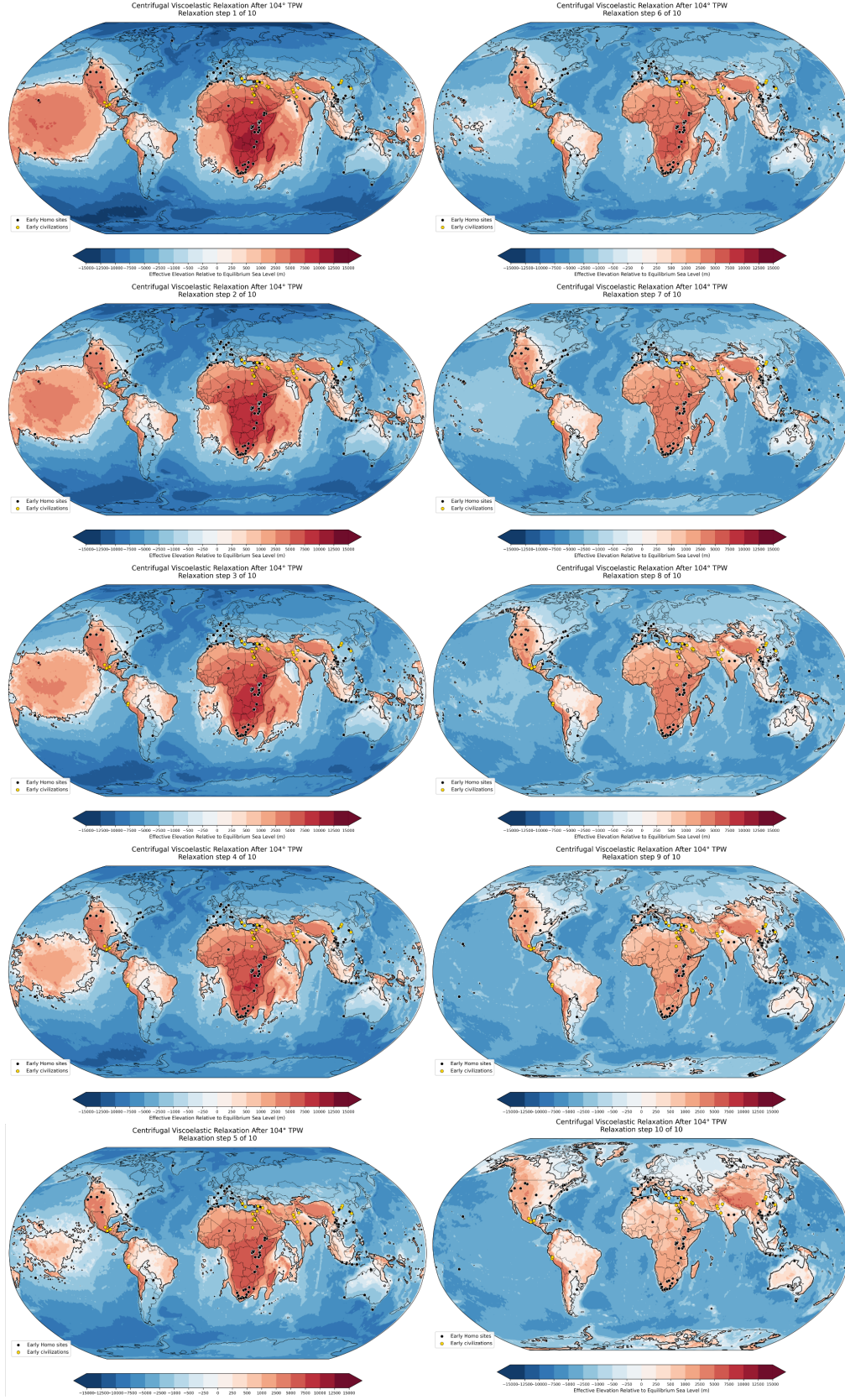
Figure 5: Ten-step centrifugal viscoelastic relaxation sequence following a 104° true polar wander event. Colors indicate effective elevation relative to equilibrium sea level. Black points denote early *Homo* sites; yellow points denote early civilizations.

the zero-anomaly contour. This pattern is difficult to reconcile with random site placement or preservation bias alone and instead suggests a constraint imposed by long-term surface stability.

Regions lying far from the equilibrium margin represent areas where land would remain persistently exposed under large-scale redistribution of sea level. Such regions would favor the long-term continuity of terrestrial habitats, repeated occupation, and the preservation of fossil-bearing deposits. In contrast, regions near the equilibrium margin are inherently more marginal, where modest perturbations could alternately expose or inundate land, leading to greater landscape instability.

10.2   Implications for early human evolution

Early members of the genus *Homo* appear to have been restricted to the most stable emergent regions of the planet. This restriction is consistent with limited technological and behavioral buffering capacity in early hominins, who would have been more vulnerable to long-term landscape instability, waterlogging, or repeated environmental reorganization.

As *Homo* evolved increased adaptability, dispersal into more marginal environments became possible. The progressive approach of younger sites toward the equilibrium margin suggests that expanding ecological tolerance, rather than random dispersal, governed the geographic trajectory of the genus. This interpretation aligns with independent evidence for increasing technological complexity, social organization, and ecological flexibility through time.

10.3   Comparison with early civilizations

The contrasting spatial behavior of early civilizations provides additional context. Early urban and proto-urban centers tend to cluster nearer the equilibrium margin rather than deep within emergent regions. These marginal zones combine long-term land persistence with fertile soils, sediment accumulation, and hydrological dynamism, conditions favorable for agriculture and dense populations but less suitable for early hominin persistence.

Taken together, the distributions of early *Homo* and early civilizations suggest a progression from origins in robustly emergent regions toward later exploitation of marginal but productive landscapes as adaptive capacity increased.

11   Limitations and Scope

The analyses presented here are intentionally first-order and geometric in nature. The viscoelastic relaxation model does not attempt to resolve full mantle rheology, lateral viscosity variations, plate tectonics, or time-dependent sediment redistribution. Instead, it isolates the dominant effect of centrifugal potential reconfiguration following rapid true polar wander.

Several limitations should be noted. First, the timing of the hypothesized TPW event is not specified, and the relaxation steps are treated as dimensionless stages rather than absolute times. Consequently, the results should be interpreted in relative rather than chronological terms.

Second, hominin site locations are subject to preservation, discovery, and reporting biases, and represent minimum constraints on past occupation rather than exhaustive population distributions. Nonetheless, the statistical analyses explicitly test whether the observed relationships could arise from random spatial arrangements, and strongly reject that hypothesis.

Third, sea-level change is modeled purely as a consequence of centrifugal adjustment and does not incorporate glacioeustatic effects, ocean circulation, or climate feedbacks. These processes would undoubtedly modulate local conditions but would not alter the global geometric structure imposed by inertial forcing.

Despite these simplifications, the consistency between the instantaneous equilibrium analysis, the relaxation sequence, and the independent archaeological dataset suggests that the results capture a real and physically meaningful signal rather than a numerical artifact.

11.1   Future directions

Future work could extend this analysis by incorporating paleogeographic reconstructions, alternative TPW geometries, or more detailed lithospheric response models. Applying similar distance-to-margin analyses

to other hominin taxa or to independent paleoecological indicators could further test the generality of the observed pattern.

12 Conclusions

This study demonstrates that a rapid true polar wander event followed by viscoelastic centrifugal relaxation produces a structured, time-evolving global pattern of relative sea-level change with direct relevance to early human geography.

Key findings include:

- A statistically significant monotonic relationship between hominin site age and distance from the post-TPW equilibrium sea-level margin.

- A viscoelastic relaxation sequence in which this margin migrates substantially, generating transient but spatially coherent zones of emergence and inundation.

- A clear contrast between early *Homo* sites, which correlate with dynamically evolving landscapes, and early civilizations, which preferentially occupy regions of long-term emergence.

These results suggest that large-scale inertial reorganization of the Earth may have played an under-appreciated role in shaping the ecological and geographic context of human evolution. More broadly, they highlight the potential for planetary-scale physical processes to impose subtle but persistent constraints on biological and cultural history.

Future work could refine the temporal calibration of the relaxation sequence, incorporate rheologically layered Earth models, and extend the analysis to other archaeological and paleontological datasets. Nonetheless, the present results establish a quantitative and physically grounded link between true polar wander dynamics and the spatiotemporal distribution of early human activity.

References

[1] Alroy, J., et al. (2001–present). The Paleobiology Database: A community resource for paleobiological data. `https://paleobiodb.org`.

[2] Childe, V. G. (1950). The urban revolution. *Town Planning Review*, 21(1), 3–17.

[3] Trigger, B. G. (2003). *Understanding Early Civilizations*. Cambridge University Press.

[4] Smith, M. E. (2016). How can archaeologists identify early cities? *Journal of Urban History*, 42(5), 845–857.

[5] Plato. *Timaeus* and *Critias*. Various translations.

[6] Aristotle. *Meteorologica*.

[7] Strabo. *Geographica*.

[8] Natural Earth. Free vector and raster map data. `https://www.naturalearthdata.com`.